

^1H NMR Studies on the Cu_A Center of Nitrous Oxide Reductase from *Pseudomonas stutzeri*[†]

Richard C. Holz,^{*,‡} Marcela L. Alvarez,[§] Walter G. Zumft,^{||} and David M. Dooley^{*,§}

Department of Chemistry and Biochemistry, Utah State University, Logan, Utah 84322-0330, Department of Chemistry, Montana State University, Bozeman, Montana 59717, and Lehrstuhl für Mikrobiologie, Universität Karlsruhe, D-76128 Karlsruhe, Germany

Received March 16, 1999; Revised Manuscript Received July 8, 1999

ABSTRACT: ^1H NMR spectra of the Cu_A center of N_2OR from *Pseudomonas stutzeri*, and a mutant enzyme that contains only Cu_A , were recorded in both H_2O - and D_2O -buffered solution at pH 7.5. Several sharp, well-resolved hyperfine-shifted ^1H NMR signals were observed in the 60 to -10 ppm chemical shift range. Comparison of the native and mutant N_2OR spectra recorded in H_2O -buffered solutions indicated that several additional signals are present in the native protein spectrum. These signals are attributed to a dinuclear copper(II) center. At least two of the observed hyperfine-shifted signals associated with the dinuclear center, those at 23.0 and 13.2 ppm, are lost upon replacement of H_2O buffer with D_2O buffer. These data indicate that at least two histidine residues are ligands of a dinuclear $\text{Cu}(\text{II})$ center. Comparison of the mutant N_2OR ^1H NMR spectra recorded in H_2O and D_2O indicates that three signals, *c* (27.5 ppm), *e* (23.6 ppm), and *i* (12.4 ppm), are solvent exchangeable. The two most strongly downfield-shifted signals (*c* and *e*) are assigned to the two $\text{N}^\epsilon\text{H}$ (N-H) protons of the coordinated histidine residues, while the remaining exchangeable signal is assigned to a backbone N-H proton in close proximity to the Cu_A cluster. Signal *e* was found to decrease in intensity as the temperature was increased, indicating that proton *e* resides on a more solvent-exposed histidine residue. One-dimensional nOe studies at pH 7.5 allowed the histidine ring protons to be definitively assigned, while the remaining signals were assigned by comparison to previously reported spectra from Cu_A centers. The temperature dependence of the observed hyperfine-shifted ^1H NMR signals of mutant N_2OR were recorded over the temperature range of 276–315 K. Both Curie and anti-Curie temperature dependencies are observed for sets of hyperfine-shifted protons. Signals *a* and *h* (cysteine protons) follow anti-Curie behavior (contact shift increases with increasing temperatures), while signals *b*–*g*, *i*, and *j* (histidine protons) follow Curie behavior (contact shift decreases with increasing temperatures). Fits of the temperature dependence of the observed hyperfine-shifted signals provided the energy separation (ΔE_L) between the ground ($^2\text{B}_{3u}$) and excited ($^2\text{B}_{2u}$) states. The temperature data obtained for all of the observed hyperfine-shifted histidine ligand protons provided a ΔE_L value of $62 \pm 35 \text{ cm}^{-1}$. The temperature dependence of the observed cysteine C^βH and C^αH protons (*a* and *h*) were fit in a separate experiment providing a ΔE_L value of $585 \pm 125 \text{ cm}^{-1}$. The differences between the ΔE_L values determined by ^1H NMR spectroscopy and those determined by EPR or MCD likely arise from coupling between relatively low-frequency vibrational states and the ground and excited electronic states.

Cytochrome *c* oxidase (CcO) and nitrous oxide reductase (N_2OR) both contain an unusual copper electron transfer center, Cu_A , that appears to function in a fashion similar to that of blue copper centers (1, 2). CcO participates in cellular respiration by coupling the four-electron reduction of O_2 to H_2O to transmembrane proton pumping, while N_2OR is

involved in the alternative respiration system of denitrifying bacteria by reducing N_2O to N_2 . N_2OR s have been purified from several denitrifying bacteria, and in each case, their activity has been associated with the presence of copper. The N_2OR from *Pseudomonas stutzeri* has been shown to have a molecular mass of 140 kDa corresponding to a homodimer with a limiting stoichiometry of four Cu atoms per subunit (3). A variety of spectroscopic studies have indicated that two copper atoms per subunit form a Cu_A type center while the remaining two copper atoms per subunit probably reside in an antiferromagnetically coupled dinuclear copper(II) site (4–19). The unusual seven-line EPR¹ signal of native N_2OR , which has been attributed to the delocalization of an unpaired electron between the two copper nuclei in the Cu_A site (4), has also been observed for intact CcO at frequencies

[†] This work was supported by the National Science Foundation (Grant CHE-9816487 to R.C.H. and Grant MCB-9723715 to D.M.D.), the National Institutes of Health (Grant GM-56495 to R.C.H.), and the Deutsche Forschungsgemeinschaft (W.G.Z.). The Bruker ARX-400 NMR spectrometer was purchased with funds provided by the National Science Foundation (Grant CHE-9311730 to R.C.H.) and Utah State University.

^{*} To whom correspondence should be addressed: Department of Chemistry and Biochemistry, Utah State University, Logan, UT 84322-0300. Phone: (435) 797-2609. Fax: (435) 797-3390. E-mail: rholz@cc.usu.edu.

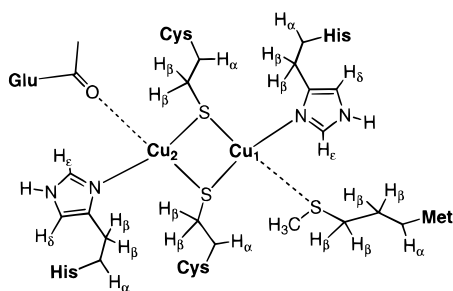
[‡] Utah State University.

[§] Montana State University.

^{||} Universität Karlsruhe.

¹ Abbreviations: ^1H NMR, proton nuclear magnetic resonance; EPR, electron paramagnetic resonance; Tris, tris(hydroxymethyl)aminomethane; nOe, nuclear Overhauser effect.

Chart 1



below X-band (6). Furthermore, a Cu—Cu distance of ~ 2.5 Å in the Cu_A center has been determined by EXAFS (20). These data suggested the presence of a Cu—Cu bonding interaction in Cu_A, which was recently substantiated in an elegant analysis of the electronic absorption, MCD, and sulfur K-edge EXAFS spectra for both CcO and several Cu_A model complexes (21, 22).

X-ray crystallographic studies on mammalian and bacterial CcO as well as the soluble domain of subunit II of the cytochrome *ba*₃ quinol oxidase have revealed the basic structural properties of the Cu_A center (7–10). Each of these structures indicated that Cu_A is a dicopper center in which each copper ion resides in a distorted four-coordinate environment. Both copper ions are bridged by two thiolate sulfur cysteine ligands (Chart 1), and each copper ion is in turn coordinated by terminal N^δ-bound histidine ligands that are trans to each other. One copper ion is further coordinated by a methionine sulfur ligand, while the second copper ion is bound by a backbone carbonyl oxygen atom of a glutamic acid residue. The nearly symmetric nature of the dicopper center, the short metal–metal distance, and the unusual spectroscopic properties indicate that Cu_A is in fact a paramagnetic ($S = 1/2$), fully delocalized [Cu(1.5)···LCu(1.5)] center. Moreover, these X-ray crystallographic studies demonstrate a structural relationship between the Cu_A center in the soluble domain of subunit II of the cytochrome *ba*₃ quinol oxidase and type I blue copper proteins (cupredoxins). Using protein engineering techniques, the blue copper sites of amicyanin and azurin have been replaced with Cu_A binding loops. These blue copper mutants provide Cu_A-type centers as shown by spectroscopic and X-ray crystallographic techniques (23–26).

Proton NMR spectroscopy is a useful technique for probing the ligand environment of coupled paramagnetic metals in multinuclear clusters (27–32). Only protons proximate to the metal cluster are shifted out of the diamagnetic envelope, providing a fingerprint of the metal ligand environment. In addition, a wealth of information about the energy separation of the ground and first excited states can be obtained by assessing the temperature dependence of the hyperfine-shifted signals (27, 28, 31, 32). Studies of this type allow the local spin magnetization to be characterized without interference from the bulk susceptibility. Proton NMR spectra of the soluble Cu_A domain from *Thermus thermophilus* cytochrome *ba*₃, three cytochrome *c* oxidases, and the Cu_A variant of amicyanin have recently been reported (33–37). Several relatively sharp, well-resolved hyperfine-shifted ¹H NMR signals were observed in the 300 to –10 ppm chemical shift range for *T. thermophilus* as well as the cytochrome *c* oxidases from

Paracoccus denitrificans and *Paracoccus versutus*. On the other hand, the Cu_A variant of amicyanin and the cytochrome *c* oxidase from *Bacillus subtilis* exhibited hyperfine-shifted signals only between 110 and –10 ppm. Several of the observed hyperfine-shifted signals in each system were assigned by both one- and two-dimensional methods, providing new insight into the electronic properties of the Cu_A center.

In an effort to gain insight into the structure and function of the Cu_A center of N₂OR from *P. stutzeri*, we have recorded the ¹H NMR spectra of native N₂OR and a mutant enzyme that contains only Cu_A (3). Nuclear Overhauser effect (nOe) difference spectra in combination with T_1 values have facilitated the assignment of several of the hyperfine-shifted ¹H NMR resonances. The temperature dependence of each hyperfine-shifted signal was also determined, and analysis of these data provides the thermal accessibility of the excited state at room temperature. These studies provide new insight into the ability of Cu_A to function in the electron-transfer pathway of denitrifying bacteria.

MATERIALS AND METHODS

Enzyme Purification. All chemicals used in this study were purchased commercially and were of the highest quality available. Native N₂OR was isolated and purified anaerobically from *P. stutzeri* (ATCC 14405) as previously described (2, 3). Mutant N₂OR was expressed in strain MK402 of *P. stutzeri*, which is defective in the biosynthesis of the catalytic center (38), and was purified aerobically as described previously (3). Protein samples were prepared in 25 mM Tris-HCl buffer (pH 7.5) in both H₂O and D₂O; the latter samples were prepared by exchanging (five times) 3 mL of D₂O buffer (99.9%) against H₂O buffer and reconcentrating the sample in an Amicon Centricon-10 microconcentrator. Each N₂OR sample was concentrated to ~ 2 mM (total enzyme concentration) in an Amicon Centricon-10 microconcentrator at pH 7.5.

Physical Methods. Proton NMR spectra were recorded on a Bruker ARX-400 spectrometer at 400.13 MHz. A presaturation pulse sequence was used to suppress the water signal and the resonances in the diamagnetic region. The pulse sequence repetition rate was typically 5 s^{–1} with a spectral window of 83 kHz. Chemical shifts (in parts per million) were referenced to the residual water peak at 4.7 ppm. The ¹H NMR data were Fourier transformed with an exponential apodization function as well as the application of a 30 Hz line broadening. Longitudinal relaxation times (T_1) were measured by using an inversion–recovery pulse sequence (180°– t –90°). Plots of $\ln(I_0 - I_t)$ versus t for each signal provided a straight line over all the t values that were investigated. Peak areas were determined as relative areas based on 1:1 ratios with signals *b* and *e* (vide infra). Non-baseline-subtracted spectra were used to determine these areas by the cut-and-weigh method. Nuclear Overhauser effect (nOe) difference spectra were obtained at 300 K by computer manipulation of the free induction decay with the saturation pulse set alternatively on the signal of interest and a reference position (100 ppm) for 10 ms. The steady state nOe (η_{ij}) on signal *i* when signal *j* is saturated for a period of time t in paramagnetic metalloproteins is given by

$$\eta_{ij} = \sigma_{ij}/\rho_i = -0.1\gamma^4 h^2 r_{ij}^{-6} t_c T_1 \quad (1)$$

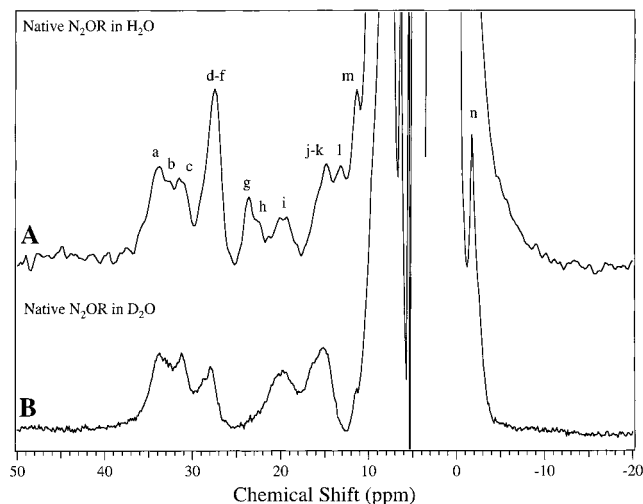


FIGURE 1: ^1H NMR spectra of (A) a 2 mM sample of native N_2OR in H_2O at 300 K and (B) a 2 mM sample of native N_2OR in D_2O at 300 K.

where σ_{ij} is the cross-relaxation between i and j , t_c is the rotational correlation time of the molecule, $r_i(T_1)$ is the spin-lattice relaxation rate of proton i , and r_{ij} is the distance between nuclei i and j . The remaining constants have their usual meaning. The decoupler was calibrated as previously described, so decoupler power spillover did not occur under the pulsing conditions used for hyperfine-shifted ^1H NMR resonances separated by ≥ 2 ppm (39).

RESULTS

^1H NMR Spectra of Native N_2OR from *P. stutzeri* at pH 7.5. The ^1H NMR spectra of N_2OR in 25 mM Tris-HCl buffer (pH 7.5) in both H_2O and D_2O solutions are shown in Figure 1. Several sharp, well-resolved hyperfine-shifted ^1H NMR signals are observed in the 40 to -10 ppm chemical shift range. Hyperfine-shifted protons in this chemical shift range have previously been observed for proteins containing Cu_A clusters and were assigned to N-H and C-H protons of cluster histidine and cysteinyl ligands (33–37). Comparison of the N_2OR spectra recorded in H_2O - and D_2O -buffered solution indicates that five hyperfine-shifted signals, e (27.5 ppm), g (23.6 ppm), h (23.0 ppm), l (13.2 ppm), and m (12.4 ppm), are solvent exchangeable (Figure 1). Since only two histidine residues reside at the Cu_A site, two of these signals are likely due to the N-H protons of the two N^δ -coordinated histidine residues. The remaining exchangeable signals are due to either backbone N-H protons in close proximity to the Cu_A cluster or N-H histidine protons of a dinuclear copper(II) center (40). Careful inspection of the 400–100 ppm chemical shift region revealed no hyperfine-shifted signals, similar to the findings for the Cu_A variant of amicyanin and the Cu_A center of *B. subtilis*. However, this is in contrast to the NMR spectra of the Cu_A centers in *T. thermophilus*, *Pa. denitrificans*, and *Pa. versutus*, where C^βH protons of the cluster cysteinyl ligands were observed (33–37).

^1H NMR Spectra of Mutant N_2OR from *P. stutzeri* at pH 7.5. The ^1H NMR spectra of mutant N_2OR in 25 mM Tris-HCl buffer (pH 7.5) in both H_2O and D_2O solutions at 300 K are shown in Figure 2 (Table 1). The ^1H NMR spectrum of the mutant enzyme exhibits fewer hyperfine-shifted signals than that of native N_2OR , due to the absence of the dinuclear

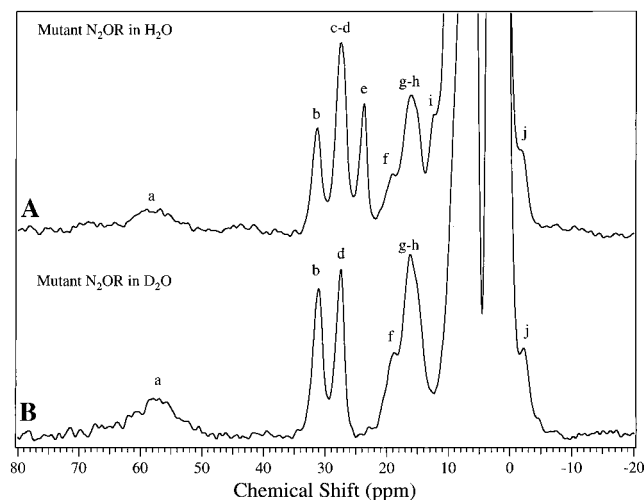


FIGURE 2: ^1H NMR spectra of (A) a 2 mM sample of mutant N_2OR in H_2O at 300 K and (B) a 2 mM sample of mutant N_2OR in D_2O at 300 K.

Table 1: Properties of the Observed Hyperfine-Shifted ^1H NMR Resonances of the Cu_A Center of Nitrous Oxide Reductase from *P. stutzeri*

signal	assignment	chemical shift (ppm) ^a	line width ^b (Hz)	relative area ^c	T_1 ^d (ms)	temperature dependence
<i>a</i>	Cys C^βH	57	3500	~ 1	< 1	anti-Curie
<i>b</i>	His ₁ $\text{C}^{\delta 2}\text{H}$	31.1	600	1	6	Curie
<i>c</i> ^e	His ₁ $\text{N}^{\epsilon}\text{H}$	27.5	ND ^f	1	ND ^f	Curie
<i>d</i>	His ₂ $\text{C}^{\delta 2}\text{H}$	27.5	730	1	6	Curie
<i>e</i> ^e	His ₂ $\text{N}^{\epsilon}\text{H}$	23.5	370	1	ND ^f	Curie
<i>f</i>	His ₁ $\text{C}^{\epsilon 1}\text{H}$	18.9	300	1	3	Curie
<i>g</i>	His ₂ $\text{C}^{\epsilon 1}\text{H}$	16.4	1000	2	< 1	Curie
<i>h</i>	Cys $\text{C}^{\alpha}\text{H}$	15.4	ND ^f	ND ^f	2	anti-Curie
<i>i</i> ^e	peptide N-H	12.4	300	ND ^f	ND ^f	Curie
<i>j</i>	His C^βH (?)	-2.1	600	1	1	Curie

^a All chemical shifts are in parts per million relative to the residual solvent signal at 4.7 ppm for H_2O . ^b Full width at half-maximum. ^c Relative areas are based on the area of signals *b* and *c*. ^d T_1 values were obtained at 400 MHz and 27 °C. ^e Solvent exchangeable. ^f Not determined.

$\text{Cu}(\text{II})$ centers in the mutant enzyme (40). The T_1 values of all of the observed signals for mutant N_2OR are in the 1–6 ms range (Table 1). Comparison of the mutant N_2OR ^1H NMR spectra recorded in H_2O and D_2O indicates that three signals, *c* (27.5 ppm), *e* (23.6 ppm), and *i* (12.4 ppm), are solvent exchangeable. The two most strongly downfield-shifted signals (*c* and *e*) are assigned to the two $\text{N}^{\epsilon}\text{H}$ (N-H) protons of the coordinated histidine residues, while the remaining exchangeable signal is assigned to a backbone N-H proton in close proximity to the Cu_A cluster. The intensity of signal *e* was found to decrease as the temperature was increased, like that of the solvent exchangeable signals in *T. thermophilus*, *Pa. denitrificans*, and *Pa. versutus* which were assigned, in each case, to a more solvent-exposed histidine residue. Thus, one of the histidine residues in N_2OR also appears to be more solvent-exposed than the other.

The ^1H NMR spectrum of mutant N_2OR is similar with respect to the chemical shifts of the observed protons to those reported for the Cu_A centers from *B. subtilis*, *T. thermophilus*, *Pa. denitrificans*, and *Pa. versutus* as well as the Cu_A variant of amicyanin (33–37). Therefore, tentative assignments of the observed hyperfine-shifted signals of mutant N_2OR may

be derived by comparison of the chemical shift, T_1 values ($\propto r_{\text{Cu-H}}^6$), relative integrations, and the temperature dependence (Table 1) to each of the previously reported ¹H NMR spectra of Cu_A centers. Comparison of signals *d* (116 ppm) and *g* (27.4 ppm) of the Cu_A domain of *T. thermophilus* with signals *a* (57 ppm) and *h* (15.4 ppm) of mutant N₂OR shows they are consistent with the assignment of these signals as Cys C^βH and C^αH protons, respectively. Likewise, comparison of signals *e* (31.7 ppm, His181 C^{δ2}H), *f* (27.7 ppm, His224 C^{δ2}H), *h* (24.4 ppm, His181 N^{ε2}H), *i* (23.3 ppm, His224 N^{ε2}H), *j* (21.1 ppm, His181 C^{ε1}H), and *k* (15.7 ppm, His224 C^{ε1}H) of the Cu_A center from *T. thermophilus* with those of mutant N₂OR shows they are consistent with the assignment of signals *b* (31.1 ppm), *d* (27.5 ppm), *c* (27.5 ppm, His₁ N^{ε2}H), *e* (23.5 ppm, His₂ N^{ε2}H), *f* (18.9 ppm), and *g* (16.4 ppm) to histidine ring protons. Similar assignments have been made for the Cu_A domains of *Pa. denitrificans* and *Pa. versutus*. The only remaining ¹H NMR resonance of mutant N₂OR is signal *j* (−2.1 ppm) which we propose to be either a His C^βH or Met C^βH proton similar to signal *y* or *n* (−2.8 ppm) of the Cu_A centers from *T. thermophilus* and *Pa. versutus*, respectively, and signal *f* (−1.3 ppm) of the Cu_A variant of amicyanin.

nOe Difference Spectra of Mutant N₂OR from *P. stutzeri* at pH 7.5. Assignment of several of the hyperfine-shifted signals was achieved by nuclear Overhauser effect (nOe) difference experiments. For paramagnetic metalloproteins with favorably short electron spin relaxation times, the steady state nOe has been shown to be a useful tool for identifying pairs of nuclei in close proximity to one another (27, 31, 32). In several attempts to obtain two-dimensional NOESY spectra, no cross signals were observed, probably because all of the observed resonances have very short T_1 values (<6 ms). Therefore, steady state nOe methods were used to assign the observed hyperfine-shifted signals of mutant N₂OR instead of two-dimensional methods. All nOe experiments with mutant N₂OR were performed in H₂O-buffered solution [25 mM Tris-HCl buffer (pH 7.5)] at 300 K. A mixing time of 10 ms was used in all experiments since the use of longer mixing times allowed spin diffusion to occur which provided unreliable nOe difference spectra. Irradiation of signal *a* showed no detectable nOe cross-relaxation to any other observed signal. This is consistent with its previous assignment to a Cys C^βH proton. On the other hand, irradiation of signal *b* showed clear cross-relaxation to the solvent exchangeable signal *c*, indicating that these two protons are in close proximity to one another (Figure 3D). An analogous nOe experiment with mutant N₂OR in D₂O at 300 K was performed in which signal *b* was selectively irradiated; no detectable nOe cross-relaxation was observed to signal *d*, thus defining signals *b* and *c* as a cross-relaxation pair. Therefore, protons *b* and *c* can be assigned to a pair of protons, His₁ C^{δ2}H and His₁ N^{ε2}H. Similarly, irradiation of the solvent exchangeable signal *e* showed clear cross-relaxation to signal *d*, indicating that these two protons are in close proximity to one another (Figure 3C). These data indicate that protons *e* and *d* make up a second pair of protons, His₂ C^{δ2}H and His₂ N^{ε2}H. Saturation of signals *g* and *h* simultaneously revealed clear nOe cross-relaxation to signal *e* (Figure 3B). Since signal *h* follows anti-Curie behavior, similar to signal *a* which has been tentatively assigned to a Cys C^{β2}H proton, it is likely that *h* is the Cys

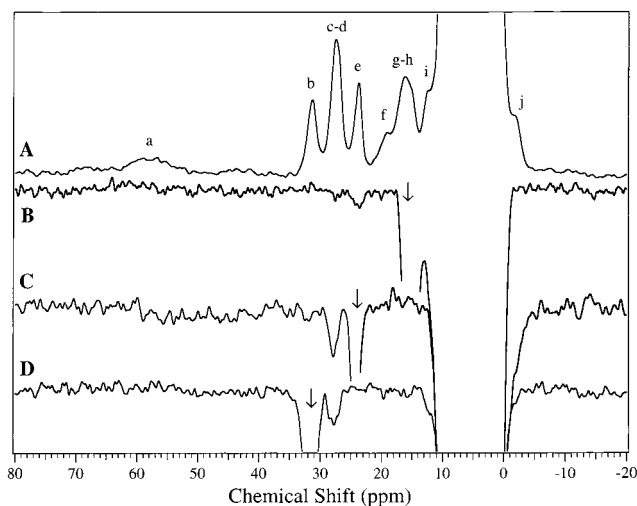


FIGURE 3: nOe difference ¹H NMR spectra of a 2 mM sample of mutant N₂OR in H₂O at 300 K with the on-resonance decoupler pulse set at the frequency denoted by the arrow. (A) ¹H NMR spectrum of a 2 mM sample of mutant N₂OR in H₂O at 300 K in 25 mM Tris-HCl buffer at pH 7.5, (B) nOe difference spectrum with the decoupler pulse centered at 16 ppm, (C) nOe difference spectrum with the decoupler pulse centered at 23.5 ppm, and (D) nOe difference spectrum with the decoupler pulse centered at 31.1 ppm.

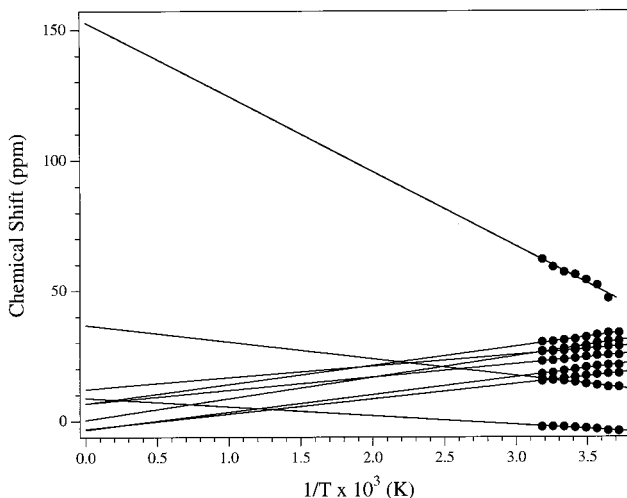


FIGURE 4: Temperature dependence of the hyperfine-shifted ¹H NMR resonances of a 2 mM sample of mutant N₂OR in D₂O in 25 mM Tris-HCl buffer at pH 7.5.

C^αH proton. Therefore, signal *g* is assigned to the His₂ C^{ε1}H proton. The corresponding C^{β2}H and C^αH protons of the coordinated histidine ligands were not observed and are likely within the diamagnetic envelope (31).

Temperature Studies. The temperature dependencies of the observed hyperfine-shifted ¹H NMR signals of mutant N₂OR were recorded over the temperature range of 276–315 K and are shown as a Curie plot in Figure 4. Both Curie and anti-Curie temperature dependencies are observed for sets of hyperfine-shifted protons. Similar observations have been made for all of the Cu_A centers studied to date by ¹H NMR spectroscopy (33–37). Signals *a* and *h* follow anti-Curie behavior (contact shift increases with increasing temperatures), while signals *b–g*, *i*, and *j* follow Curie behavior (contact shift decreases with increasing temperatures). The anomalous temperature behavior of signals *a* and *h*, both of which belong to bridging cysteine ligand protons,

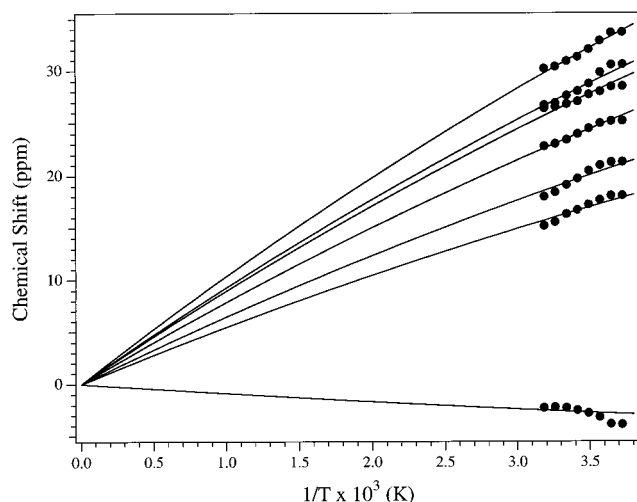


FIGURE 5: Fits of the temperature dependence of the hyperfine-shifted histidine protons of a 2 mM sample of mutant N₂OR in D₂O in 25 mM Tris-HCl buffer at pH 7.5 between 276 and 308 K.

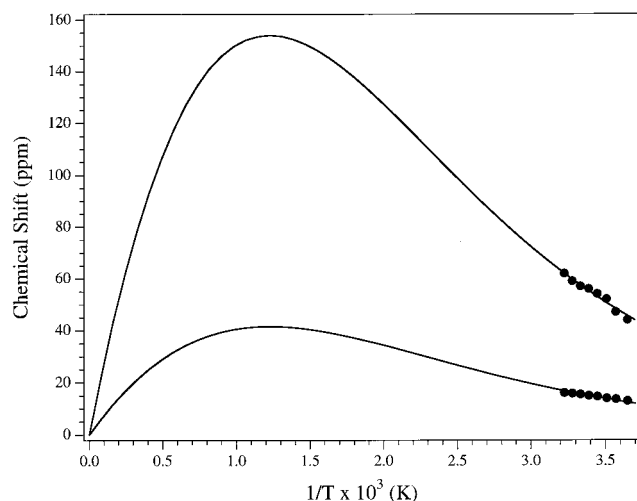


FIGURE 6: Fits of the temperature dependence of the hyperfine-shifted cysteine protons of a 2 mM sample of mutant N₂OR in D₂O in 25 mM Tris-HCl buffer at pH 7.5 between 276 and 308 K.

has been previously ascribed to distinct orbital interactions of the bridging sulfur atom with each copper ion (35–37). Inspection of Figure 4 reveals that the temperature dependencies of the hyperfine-shifted signals in which the contact shift decreases with increasing temperatures do not strictly follow Curie behavior (41). Deviations of hyperfine shift from Curie law can be understood by considering the presence of two closely spaced energy levels where the differences between the ground and excited states are on the order of kT . The electronic relaxation rate enhancement for Cu_A centers has previously been postulated to be the result of two low-lying doublets that are spaced by $\leq 6kT$ for an Orbach process or slightly more for a Raman process (35–37).

In an elegant study by Shokhirev and Walker (42), the temperature dependencies of hyperfine-shifted signals for multilevel systems were described. Their approach takes into account the temperature-dependent change in the population of the excited state which allowed accurate simulation of the temperature dependence of the hyperfine-shifted signals for several low-spin Fe(III) model hemes and heme proteins (43, 44). This approach has also been used to evaluate the

strength of the spin-coupling interaction for 2Fe-2S clusters as well as dicopper(II) centers (40, 45). For a two-level case, such as that found for Cu_A centers, the energy separation ΔE_L (where $\Delta E_L = E_2 - E_1$) between the ground state and the first excited state can be determined (40, 45). The temperature data obtained for all of the observed hyperfine-shifted histidine ligand protons for mutant N₂OR were simultaneously fit (Figure 5) using the program TDF21LVL kindly provided by N. Shokhirev and A. Walker (42). These fits provided a ΔE_L value of $62 \pm 35 \text{ cm}^{-1}$. In a separate experiment, the temperature dependencies of the observed cysteine C β H and C α H protons (*a* and *h*), which exhibit anti-Curie behavior, were fit (Figure 6), and a ΔE_L value of $585 \pm 125 \text{ cm}^{-1}$ was determined. The significant errors associated with both of these fits are the result of fitting only a small temperature range, as dictated by protein stability and solvent. Additional errors are incurred for the fit of the cysteine protons because only two resonances are fit simultaneously.

DISCUSSION

Until a few years ago, ¹H NMR spectroscopy was largely overlooked as a probe of dicopper centers in biological systems. This lack of attention stems from the fact that mononuclear copper(II) ions exhibit long electronic relaxation times, thus making them poor paramagnetic ¹H NMR probes (28). Therefore, the fact that relatively sharp hyperfine-shifted signals are observed from mixed-valent Cu_A centers suggests an alternative electronic relaxation pathway. From ¹H NMR relaxation data reported by Bertini et al. (35), a room-temperature electron relaxation rate of $\sim 10^{11} \text{ s}^{-1}$ for Cu_A was determined. This rate can be compared to those of mononuclear Cu(II) centers which have electronic relaxation rates of $\sim 10^8\text{--}10^9 \text{ s}^{-1}$ (28). Increased electronic relaxation rates have also been observed for spin-coupled dicopper(II) centers, and consequently, relatively sharp, hyperfine-shifted ¹H NMR signals are observed (46–55). For dicopper(II) systems, the nuclear relaxation rate enhancements are all decreased by a factor of 2 because of spin coupling between the two metal ions (54). Antiferromagnetic coupling, for example, creates a dicopper(II) system in which the ground ($S = 0$) state is separated from the first excited ($S = 1$) state by the exchange constant, $2J$ (51, 56). Therefore, two low-lying energy levels that provide a facile electronic relaxation pathway are present (52, 54).

Several well-resolved resonances are observed in the ¹H NMR spectrum of native N₂OR in the 40 to -10 chemical shift range. Some of these signals are absent in the mutant N₂OR enzyme. Since spin-coupled dinuclear copper(II) centers exhibit relatively sharp, hyperfine-shifted signals, the extra signals observed for native N₂OR are ascribed to a dinuclear copper(II) center. Magnetic susceptibility studies established that the Cu_A center in N₂OR from *P. stutzeri* is the only paramagnetic center in the enzyme, and that the remaining copper ions are either strongly antiferromagnetically coupled ($\geq 200 \text{ cm}^{-1}$) or Cu(I) (13). The NMR results are clearly consistent only with the former. There are two possibilities for the identity of the dinuclear Cu(II) center. It may be the oxidized form of the catalytic site. Reduction of the Cu_A center in N₂OR reveals low-energy electronic transitions associated with an EPR-silent Cu(II) center, designated Cu_Z (14). Cu_Z has been suggested to be the catalytic site, where nitrous oxide is reduced to dinitrogen.

Alternatively, Farrar et al. (16) have recently suggested that Cu_Z is a variant $[\text{Cu}(\text{II})\cdot\text{Cu}(\text{II})]$ form of Cu_A , which may be found in nitrous oxide reductase but not in cytochrome oxidase (16). Regardless, at least two of the observed hyperfine-shifted signals due to the dinuclear $\text{Cu}(\text{II})$ center (either Cu_Z or a distinct catalytic site), those at 23.0 and 13.2 ppm, are lost upon replacement of H_2O buffer with D_2O buffer. Comparison of the chemical shifts of these two resonances with relevant ^1H NMR data from synthetic model and enzyme studies (40, 52) suggests that they are due to histidine N-H protons. Therefore, if these resonances are associated with the catalytic center in N_2OR , it must have at least two histidine residues. Certainly, there are several conserved histidines in addition to the Cu_A ligands among N_2OR s from various sources.

Comparison of data for mutant N_2OR with ^1H NMR data reported for the Cu_A centers from *B. subtilis*, *T. thermophilus*, *Pa. denitrificans*, and *Pa. versutus* as well as the Cu_A variant of amicyanin (33–37) reveals several similarities and differences. Mutant N_2OR from *P. stutzeri* exhibits several well-resolved hyperfine-shifted ^1H NMR resonances in the 35 to -10 ppm chemical shift range arising from ligand protons at the Cu_A cluster. The smaller chemical shift range observed for mutant N_2OR compared to those of other Cu_A centers indicates a slightly greater degree of delocalization of the unpaired electron between the two copper ions of the Cu_A center. On the basis of EPR studies, $\sim 39\%$ of the electron density is delocalized between the two copper ions of the Cu_A center of N_2OR (18). Moreover, all of the ^1H NMR line widths of mutant N_2OR are 5–10 times larger than those reported for other Cu_A centers (Table 1). Similarly, all of the observed T_1 values are 2–10 times shorter than those reported for hyperfine-shifted signals of other Cu_A centers. Both of these observations likely result from the large physical size of the N_2OR from *P. stutzeri* (140 kDa) which increases the tumbling time (τ_r) of the enzyme. These properties make signal assignment by two-dimensional methods difficult; therefore, one-dimensional steady state nOe methods were used to assign several of the observed hyperfine-shifted signals for mutant N_2OR .

All of the resonances observed in the 35 to -10 ppm chemical shift range for mutant N_2OR were assigned to histidine ligand protons except one; signal *h* (15.4 ppm) was assigned to a Cys C^αH . Similar assignments were made for Cu_A centers from *B. subtilis*, *T. thermophilus*, *Pa. denitrificans*, and *Pa. versutus* as well as for the Cu_A variant of amicyanin (33–37). For the soluble Cu_A domain from *T. thermophilus*, the signal at 27.4 ppm was assigned to a bridging Cys C^αH proton. Similar assignments were made for the resonances observed at 23.8 ppm for the *Pa. denitrificans* and 23.4 ppm for the *Pa. versutus* Cu_A centers. The corresponding resonance observed for the Cu_A variant of amicyanin was alternatively assigned to the $\text{C}^\epsilon\text{H}$ proton of a coordinated histidine ligand; however, the authors point out that the assignment of this resonance to a Cys C^αH proton cannot be ruled out. For mutant N_2OR , the two observed exchangeable signals indicate that the two histidine ligands reside in nonequivalent sites at the Cu_A center and one, signal *e*, is more solvent-exposed. A recent model (57) for the C-terminal Cu_A domain of N_2OR from *Achromobacter cycloclastes* predicted that one histidine (H628) is more exposed to solvent (Figure 7). This histidine is located

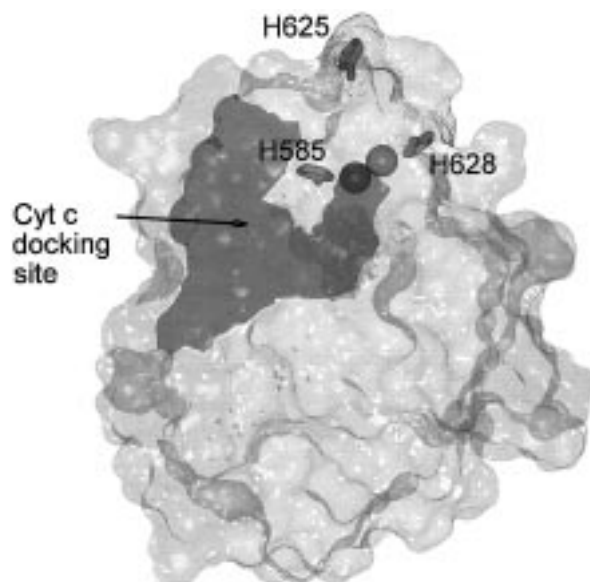


FIGURE 7: Model of the Cu_A domain of nitrous oxide reductase. The predicted protein surface is shown. That part of the domain surface associated with the acidic residues that make up the presumed cytochrome *c* binding site is shown in dark gray. In addition, the domain surfaces associated with H625 and H628 are shown as a dotted region. H625 is located at the predicted interface between the Cu_A domain and the remainder of the nitrous oxide reductase protein and, therefore, is not exposed to solvent. H628 is predicted to be partially solvent-exposed, whereas H585 is completely buried. Note this model was generated for the *A. cycloclastes* enzyme (see ref 55) but should be applicable to the *P. stutzeri* enzyme given the high level of sequence identity.

opposite the putative cytochrome *c* binding patch. On the other hand, H585 is predicted to be buried within the Cu_A domain. These two residues correspond to H626 and H583 in the enzyme from *P. stutzeri*. Last, the two or three resonances observed upfield (-1 to -10 ppm) in each Cu_A center studied to date were assigned to His C^βH , Met C^βH , and/or backbone amine N-H protons.

Assignment of several of the observed hyperfine-shifted ^1H NMR resonances of mutant N_2OR coupled with the temperature dependence of the hyperfine-shifted resonances allows information about the electronic properties of the Cu_A site to be obtained. Both Curie and anti-Curie temperature dependencies are observed for hyperfine-shifted signals of mutant N_2OR . Similar results were obtained for the Cu_A centers from *B. subtilis*, *T. thermophilus*, *Pa. denitrificans*, and *Pa. versutus* as well as for the Cu_A variant of amicyanin. In each of these studies, resonances exhibiting anti-Curie behavior were assigned to bridging cysteine ligand protons. For mutant N_2OR , signals *a* and *h* were assigned to cysteine C^βH and C^αH protons due, primarily, to their anti-Curie temperature behavior. These protons exhibit anti-Curie behavior because of distinct orbital interactions of the bridging sulfur atom with each copper ion (35–37). Fits of the temperature dependence of these two resonances (*a* and *h*) result in a ΔE_L value of 585 cm^{-1} . Salgado et al. (37) obtained a ΔE_L value of 350 cm^{-1} by fitting the observed chemical shifts for the four cysteine C^βH protons of the Cu_A center from *Pa. denitrificans*. The remaining signals, all of which exhibit Curie behavior, are due to histidine ligand protons. Fits of the temperature data for each observed resonance of the histidine ligand protons of mutant N_2OR provide a ΔE_L value of 62 cm^{-1} . However, on the basis of

MCD data, the ${}^2B_{3u} \rightarrow {}^2B_{2u}$ energy separation for the Cu_A cluster of mutant N_2OR was found to be 4500 cm^{-1} , whereas that of the Cu_A center from *Pa. denitrificans* was 3500 cm^{-1} (15, 16).

Canters and co-workers (37) suggested that the discrepancy between the ΔE_L values determined by NMR spectroscopy and those determined by EPR or MCD is due to coupling between relatively low-frequency vibrational states and the ground and excited electronic states. They also pointed out that as the $Cu-S-Cu$ angle decreases, the energy gap between the ${}^2B_{3u}$ and ${}^2B_{2u}$ levels decreases. If the angle becomes acute enough (in the range of $65-70^\circ$), the ordering of the energy levels could even become reversed. $Cu-S-Cu$ angles determined from both EXAFS (20) and X-ray crystallographic studies (7–10, 26) with Cu_A centers are close to this range, suggesting that the energy separation for N_2OR is likely much smaller than 3500 cm^{-1} at room temperature. Canters and co-workers (37) also suggested that for small energy separations between the ${}^2B_{3u}$ and ${}^2B_{2u}$ levels, low-lying vibrational states could mix with the ground and excited states (37). Orbital mixing with vibrational states is confirmed by resonance Raman studies since enhancement of the Cu_2S_2 twisting vibration (ν_3) indicated that the $Cu-S$ bonding interaction is distinct for each thiolate but related to the other through an inversion center (12). From these studies, the excited state vibrational relaxation of Cu_A clusters was shown to be dominated by the accordion (ν_1) and breathing (ν_4) vibrations. The ν_1 vibration of Cu_A has an energy of $\sim 130\text{ cm}^{-1}$, whereas the ν_4 vibrations occur at $\sim 340\text{ cm}^{-1}$. The value of ν_4 is similar to the ΔE_L value obtained for the cysteine protons for mutant N_2OR as well as for the Cu_A center from *Pa. denitrificans*. Thus, the ΔE_L values of 585 and 350 cm^{-1} determined from cysteine 1H NMR temperature data appear to reflect the Cu_2S_2 breathing vibration (ν_4). On the other hand, analysis of 1H NMR temperature data for the histidine ring protons of mutant N_2OR provides a ΔE_L value of 62 cm^{-1} . This value appears to reflect the accordion vibration of the Cu_2S_2 cluster (ν_1) which is reasonable since the two histidine ligands are trans to one another, each coordinating different copper ions. Therefore, 1H NMR spectra of each of the Cu_A centers studied to date appear to reflect the accordion (ν_1) and breathing (ν_4) vibrations in the temperature dependence of their chemical shifts.

As has been discussed previously (8–10, 15–18, 21, 22, 34–37), the structure of the Cu_A site is exquisitely designed for its electron-transfer role. Solomon and co-workers have suggested that the pronounced covalency of the bonding in the Cu_2S_2 unit activates electron transfer via the bridging cysteines in Cu_A . Indeed, using a standard model (58), it was estimated that the dithiolate unit may provide effective electron-transfer pathways from cytochrome *c* to Cu_A , and from Cu_A to heme *a* (22). Examination of Figure 7 suggests that electron transfer to N_2OR Cu_A from the cytochrome binding site may proceed via H585, but there may well be a pathway via a bridging cysteine that is competitive. Interestingly, the C624-H625 motif makes an appealing electron-transfer pathway from Cu_A to the catalytic site. H625 (H623 in *P. stutzeri* N_2OR) is conserved among nitrous oxide reductases and is predicted by the model to be positioned such that it could serve as part of an electron-transfer pathway to the catalytic copper site. On the basis of similarities to

the multi-copper enzymes ascorbate oxidase and nitrite reductase, H625 is a potential catalytic site copper ligand (57). The presumed catalytic site domain in N_2OR is roughly composed of residues 133–184 (*A. cycloclastes*) and is 50% similar and 25% identical to the analogous ascorbate oxidase domain. This is identical to the sequence homology between ascorbate oxidase and nitrite reductase, where in both enzymes the Cys-His motif links the electron-transfer and catalytic centers. Furthermore, our results are consistent with the conclusion from previous spectroscopic studies that the valence delocalization and covalency of Cu_A in N_2OR are comparable to that for Cu_A in cytochrome oxidase, and ensure that the reorganization energy for electron transfer is low. Solomon and co-workers pointed out that the pronounced covalency and electronic delocalization in Cu_A may simultaneously permit the tuning of the redox potential while providing two Cu -cysteine electron-transfer pathways (22), and this is an attractive hypothesis for the role of Cu_A in N_2OR .

REFERENCES

1. Babcock, G. T., and Wikström, M. (1992) *Nature* 356, 301–309.
2. Coyle, C. L., Zumft, W. G., Kroneck, P. M. H., Körner, H., and Jakob, W. (1985) *Eur. J. Biochem.* 153, 459–467.
3. Riester, J., Zumft, W. G., and Kroneck, P. M. H. (1989) *Eur. J. Biochem.* 178, 751–762.
4. Kroneck, P. M. H., Antholine, W. A., Riester, J., and Zumft, W. G. (1988) *FEBS Lett.* 242, 70–74.
5. Dooley, D. M., McGuirl, M. A., Rosenzweig, A. C., Landin, J. A., Scott, R. A., Zumft, W. G., Devlin, F., and Stephens, P. J. (1991) *Inorg. Chem.* 30, 3006–3011.
6. Antholine, W. E., Kastrau, D. H. W., Steffens, G. C. M., Buse, G., Zumft, W. G., and Kroneck, P. M. H. (1992) *Eur. J. Biochem.* 209, 875–881.
7. Iwata, S., Ostermeier, C., Ludwig, B., and Michel, H. (1995) *Nature* 376, 660–669.
8. Wilmanns, M., Lappalainen, P., Kelly, M., Sauer-Eriksson, E., and Saraste, M. (1995) *Proc. Natl. Acad. Sci. U.S.A.* 92, 11955–11959.
9. Tsukihara, T., Aoyama, H., Yamashita, E., Tomizaki, T., Yamaguchi, H., Shinzawa-Itoh, K., Nakashima, R., Yaono, R., and Yoshikawa, S. (1995) *Science* 269, 1069–1074.
10. Tsukihara, T., Aoyama, H., Yamashita, E., Tomizaki, T., Yamaguchi, H., Shinzawa-Itoh, K., Nakashima, R., Yaono, R., and Yoshikawa, S. (1996) *Science* 272, 1136–1144.
11. Scott, R. A., Zumft, W. G., Coyle, C. L., and Dooley, D. M. (1989) *Proc. Natl. Acad. Sci. U.S.A.* 86, 4082–4086.
12. Dooley, D. M., Moog, R. S., and Zumft, W. G. (1987) *J. Am. Chem. Soc.* 109, 6730–6735.
13. Dooley, D. M., Landin, J. A., Rosenzweig, A. C., Zumft, W. G., and Day, E. P. (1991) *J. Am. Chem. Soc.* 113, 8978–8980.
14. Farrar, J. A., Thompson, A. J., Cheesman, M. R., Dooley, D. M., and Zumft, W. G. (1991) *FEBS Lett.* 294, 11–15.
15. Farrar, J. A., Neese, F., Lappalainen, P., Kroneck, P. M. H., Saraste, M., Zumft, W. G., and Thompson, A. J. (1996) *J. Am. Chem. Soc.* 118, 11501–11514.
16. Farrar, J. A., Zumft, W. G., and Thompson, A. J. (1998) *Proc. Natl. Acad. Sci. U.S.A.* 95, 9891–9896.
17. Andrew, C. R., Han, J., de Vries, S., van der Oost, J., Averill, B. A., Loehr, T. M., and Sanders-Loehr, J. (1994) *J. Am. Chem. Soc.* 116, 10805–10806.
18. Neese, F., Zumft, W. G., Antholine, W. E., and Kroneck, P. M. H. (1996) *J. Am. Chem. Soc.* 118, 8692–8699.
19. Neese, F., Kappl, R., Hüttermann, J., Zumft, W. G., and Kroneck, P. M. H. (1998) *JBIC, J. Biol. Inorg. Chem.* 3, 53–67.
20. Blackburn, N. J., Barr, M. E., Woodruff, W. H., van der Oost, J., and de Vries, S. (1994) *Biochemistry* 33, 10401–10407.

21. Williams, K. R., Gamelin, D. R., LaCroix, L. B., Houser, R. P., Tolman, W. B., Mulder, T. C., de Vries, S., Hedman, B., Hodgson, K. O., and Solomon, E. I. (1997) *J. Am. Chem. Soc.* **119**, 613–614.
22. Gamelin, E. R., Randall, D. W., Hay, M. T., Houser, R. P., Mulder, T. C., Canters, G. W., de Vries, S., Tolman, W. B., Lu, Y., and Solomon, E. I. (1998) *J. Am. Chem. Soc.* **120**, 5246–5263.
23. Andrew, C. R., Lappalainen, P., Saraste, M., Hay, M. T., Lu, Y., Dennison, C., Canters, G. W., Fee, J. A., Slutter, C. E., Nakamura, N., and Sanders-Loehr, J. (1995) *J. Am. Chem. Soc.* **117**, 10759–10760.
24. Dennison, C., Vijgenboom, E., de Vries, S., van der Oost, J., and Canters, G. W. (1995) *FEBS Lett.* **365**, 92–94.
25. Hay, M. T., Richards, J. H., and Lu, Y. (1996) *Proc. Natl. Acad. Sci. U.S.A.* **93**, 461–464.
26. Robinson, H., Ang, M. C., Gao, Y.-G., Hay, M. T., Lu, Y., and Wang, H. H.-J. (1999) *Biochemistry* **38**, 5677–5683.
27. La Mar, G. N., and de Ropp, J. S. (1993) in *Biological Magnetic Resonance: NMR of Paramagnetic Molecules* (Berliner, L. J., and Reuben, J., Eds.) pp 1–78, Plenum Press, New York.
28. Bertini, I., and Luchinat, C. (1986) *NMR of Paramagnetic Molecules in Biological Systems*, Benjamin & Cummings, Menlo Park, CA.
29. Bertini, I., Molinari, N., and Niccolai, N. (1991) *NMR and Biomolecular Structure*, VCH, New York.
30. Bertini, I., and Luchinat, C. (1992) in *Physical Methods for Chemists* (Drago, R. S., Ed.) pp 500–556, Harcourt Brace Jovanovich, Orlando, FL.
31. Bertini, I., Turano, P., and Vila, A. J. (1993) *Chem. Rev.* **93**, 2833–2932.
32. Cheng, H., and Markley, J. L. (1995) *Annu. Rev. Biophys. Biomol. Struct.* **24**, 209–237.
33. Dennison, C., Berg, A., de Vries, S., and Canters, G. W. (1996) *FEBS Lett.* **394**, 340–344.
34. Dennison, C., Berg, A., and Canters, G. W. (1997) *Biochemistry* **36**, 3262–3269.
35. Bertini, I., Bren, K. L., Clemente, A., Fee, J. A., Gray, H. B., Luchinat, C., Malmström, B. G., Richards, J. H., Sanders, D., and Slutter, C. (1996) *J. Am. Chem. Soc.* **118**, 11658–11659.
36. Luchinat, C., Sorianio, A., Djinovic-Carugo, K., Saraste, M., Malmström, B. G., and Bertini, I. (1997) *J. Am. Chem. Soc.* **119**, 11023–11027.
37. Salgado, J., Warmerdam, G., Bubacco, L., and Canters, G. W. (1998) *Biochemistry* **37**, 7378–7389.
38. Zumft, W. G., Viebrock-Sambale, A., and Braun, C. (1990) *Eur. J. Biochem.* **192**, 591–599.
39. Lanzilotta, W. N., Holz, R. C., and Seefeldt, L. C. (1995) *Biochemistry* **34**, 15646–15653.
40. Holz, R. C., Bennett, B., Chen, G., and Ming, L.-J. (1998) *J. Am. Chem. Soc.* **120**, 6329–6335.
41. Banci, L., Bertini, I., Luchinat, C., Pierattelli, R., Shokhirev, N. V., and Walker, F. A. (1998) *J. Am. Chem. Soc.* **120**, 8472–8479.
42. Shokhirev, N. V., and Walker, F. A. (1995) *J. Phys. Chem.* **99**, 17795–17804.
43. Horrocks, W. D., and Greenberg, E. S. (1973) *Biochim. Biophys. Acta* **322**, 38–44.
44. Horrocks, W. D., and Greenberg, E. S. (1974) *Mol. Phys.* **27**, 993–999.
45. Holz, R. C., Small, F. J., and Ensign, S. A. (1997) *Biochemistry* **36**, 14690–14696.
46. Byers, W., and Williams, R. J. P. (1972) *J. Chem. Soc., Dalton Trans.*, 555–560.
47. Zelonka, R. A., and Baird, M. C. (1972) *Inorg. Chem.* **11**, 134–137.
48. Maekawa, M., Kitagawa, S., Munakata, M., and Masuda, H. (1989) *Inorg. Chem.* **28**, 1904–1909.
49. Holz, R. C., Brink, J. M., Gobena, F. T., and O'Connor, C. J. (1994) *Inorg. Chem.* **33**, 6086–6092.
50. Holz, R. C., and Brink, J. M. (1994) *Inorg. Chem.* **33**, 4609–4610.
51. Holz, R. C., Brink, J. M., and Rose, R. R. (1996) *J. Magn. Reson. A* **119**, 125–128.
52. Brink, J. M., Rose, R. R., and Holz, R. C. (1996) *Inorg. Chem.* **35**, 2878–2885.
53. Satcher, J. H., and Balch, A. L. (1995) *Inorg. Chem.* **34**, 3371–3373.
54. Murthy, N. N., Karlin, K. D., Bertini, I., and Luchinat, C. (1997) *J. Am. Chem. Soc.* **119**, 2156–2162.
55. Bubacco, L., Salgado, J., Tepper, A. W. J. W., Vijgenboom, E., and Canters, G. W. (1999) *FEBS Lett.* **442**, 215–220.
56. Drago, R. S. (1992) *Physical Methods for Chemists*, 2nd ed., Saunders, Orlando, FL.
57. McGuirl, M. A., Nelson, L. K., Bollinger, J. A., Chan, Y.-K., and Dooley, D. M. (1998) *J. Inorg. Biochem.* **70**, 155–169.
58. Beratan, J. N., Betts, J. N., and Onuchic, J. N. (1991) *Science* **252**, 1285–1288.

BI990595E